

# Shutdown Characteristics of an Axial-Groove Liquid-Trap Heat-Pipe Thermal Diode

M. Groll\* and W. Supper†

*Universität Stuttgart, Stuttgart, Federal Republic of Germany*  
and

C.J. Savage‡

*European Space Research and Technology Centre (ESTEC), Noordwijk, the Netherlands*

The shutdown characteristics of an axial-groove liquid-trap heat-pipe thermal diode made of aluminum and using ammonia as the working fluid have been theoretically and experimentally determined. The heat-pipe diode has a total length of 470 mm and an outside diameter of 10 mm (the trap dimensions are 70 mm long and 25 mm outside diameter). The shutdown technique employed consisted of heating the condenser by applying a constant heat input while having the evaporator and trap, both thermally coupled to an aluminum thermal mass, thermally free-floating. The required shutdown energy (approximately 1.2 W·h) came very close to the theoretical minimum shutdown energy of 1.48 W·h, indicating no back-piping action during shutdown. The shutdown times were strongly dependent on the shutdown power applied. They varied between about 30 and 7 min for shutdown powers of between 5 and 15 W.

## Introduction

HEAT-PIPE thermal diodes are being developed as passive thermal control elements for spacecraft temperature control.<sup>1-7</sup> They are used, for example, to prevent electronic components from being overheated by adverse heat flows in cases when the heat sink (radiator) is on a higher temperature level than the electronic component itself.

The two major heat-pipe diode techniques are the liquid-trap and the liquid-blockage techniques. The liquid-trap technique makes use of a reservoir (the liquid trap) at the evaporator end of the heat pipe. Under adverse heat-flow conditions the working fluid vapor is condensed in the heat-pipe evaporator and trap. Since there is no capillary structure connecting evaporator and trap, the vapor condensed in the trap is contained there and thus the heat pipe dries out. The adverse heat flow in the dried-out heat pipe is thereby reduced to thermal conduction in the heat-pipe wall. The liquid-blockage technique requires a liquid reservoir, filled with excess liquid, at the condenser end of the heat pipe. Under adverse heat-flow conditions this excess liquid is expelled from the reservoir and enters the heat pipe essentially as vapor. The vapor is condensed in the evaporator and collected there. Depending on the amount of excess liquid provided in the reservoir, the evaporator and a substantial part of the adiabatic heat-pipe section are blocked with liquid, thus reducing the adverse heat flow to thermal conduction in the liquid plug and in the heat-pipe wall.

Theoretical and experimental work on liquid-trap heat-pipe diodes, utilizing both the axial-groove and the artery heat-pipe concept, has been carried out and the results have been described in Refs. 5 and 7. In those experiments a shutdown technique has been employed which consisted of rapidly cooling the diode evaporator and trap while maintaining the

condenser at a constant temperature. Although in most practical applications shutdown might be accomplished by warming the condenser rather than cooling evaporator and trap, the cool-down method has been employed because it allows a rather precise determination of the shutdown characteristics, viz. shutdown time, transient shutdown power, and shutdown energy.

Additional work has been carried out since to determine the shutdown characteristics of an axial-groove liquid-trap diode employing a shutdown technique which consists of heating the condenser by applying a constant heat flux while having a thermally free-floating evaporator and trap. Respective shutdown experiments have been carried out and a simple mathematical shutdown model has been developed.

In this paper theoretical and experimental results are presented, and they are compared with results obtained with the different shutdown techniques described in Refs. 5 and 7.

## Design of Heat-Pipe Diode

For the present investigation a straight prototype heat-pipe diode, denominated P1, which had been already investigated in Refs. 5 and 7 has been used. This diode consists of an axial-groove aluminum heat pipe with a liquid trap at the evaporator end. The liquid trap employs circumferential grooves at the inner trap wall and a central slab wick supported by a perforated plate. Ammonia (4.5 g) is used as the working fluid. Figure 1 shows the cross sections of both the axial-groove heat pipe and the liquid trap. The geometrical data of the diode are summarized in Table 1.

## Test Setup, Instrumentation, and Experimental Procedure

For testing the heat-pipe diode is mounted on an optical bench using three supports. To minimize heat losses to the surroundings the diode is insulated with Armaflex insulation. Gaps in this insulation are filled with Fiberfrax insulation. In Fig. 2 a schematic of the test setup without insulation and mounting supports is shown. The diode is instrumented with a condenser heater, a deployable condenser block, an evaporator thermal mass, and a trap thermal mass. Temperatures are measured with 12 NiCr-Ni thermocouples and monitored by a 12 point recorder. The deployable condenser block is coupled to a cryostat cooling loop. The condenser heater is located beneath the condenser block and consists of

Presented as Paper 80-1483 at the AIAA 15th Thermophysics Conference, Snowmass, Colo., July 14-16, 1980; submitted Jan. 14, 1981; revision received June 15, 1981. Copyright © American Institute of Aeronautics and Astronautics, Inc., 1980. All rights reserved.

\*Head, Energy Conversion and Heat Transfer Division, Institut für Kernenergetik & Energiesysteme. Member AIAA.

†Staff Member, Energy Conversion and Heat Transfer Division, Institut für Kernenergetik & Energiesysteme.

‡Staff Member, Thermal Control Section.

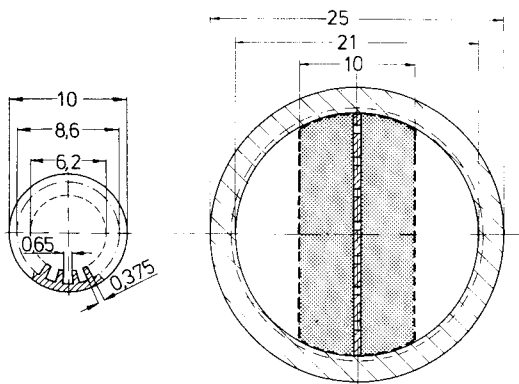


Fig. 1 Cross section of axial-groove heat pipe and liquid trap (dimensions in mm).

Table 1 Geometrical data of axial-groove aluminum heat-pipe diode

Diode	
Overall length without end pinch	470 mm
Length of evaporator	100 mm
Length of condenser	100 mm
Heat pipe	
O.d.	10 mm
I.d. (land tips)	6.2 mm
Axial grooves	19 mm
Groove opening	0.65 mm
Groove depth	1.2 mm
Trap	
O.d.	25 mm
I.d. (land tips)	21 mm
Wall thickness, trap tube	2.0 mm
trap end disks	2.5 mm
Circumferential grooves	30/cm
Groove width	0.2 mm
Groove opening angle	60 deg
Folded slab wick	160 mesh screen
Slab width	10 mm

nichrome ribbon wrapped around the pipe between two layers of Kapton foil. The heat input is provided by a stabilized direct-current source. The thermal masses for evaporator and trap are made of aluminum. They are designed in such a way that the trap block is able to absorb a thermal energy of 1.5 W·h for a temperature increase of 22 K. The evaporator block can absorb about 0.4 W·h for the same temperature increase. For an assumed shutdown energy of 1.5 W·h which corresponds to the theoretical minimum shutdown energy, the thermal mass of the trap would be able to absorb the latent heat of vaporization of the complete liquid-fill charge of the diode. The relatively small evaporator thermal mass shall assure that during shutdown the trap is always somewhat colder than the evaporator.

Both the trap and evaporator blocks are of cylindrical shape and consist of two halves which are bolted together using thermal grease. The dimensions of the trap block are 70 mm long × 50 mm o.d. × 25 mm i.d. and those of the evaporator block are 100 × 21 × 10 mm.

Before the shutdown test is started, the diode is operated in the forward mode with removed condenser insulation at a small heat load of about 10 W. This is accomplished by warming both the evaporator and trap using a fan and operating the condenser cooling loop at a coolant temperature of 15°C while the condenser block is firmly attached to the diode. Trap and evaporator temperature are increased to about 50°C. Then the fan is turned off, and both evaporator and trap start to cool. When evaporator and trap have reached a temperature of about 22°C, with

$$T_{12}, T_{11} > T_{10} > T_9 \quad \text{to} \quad T_3 > T_1 > T_2 \quad (T_2 \approx 18.5^\circ\text{C})$$

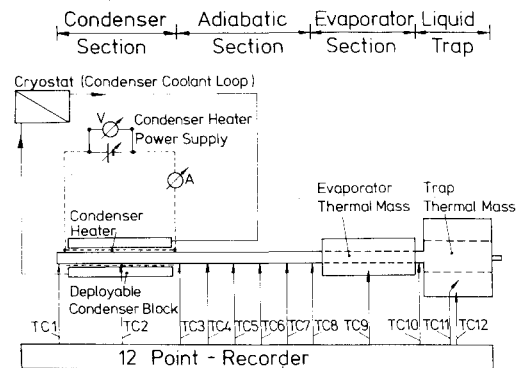


Fig. 2 Schematic of test setup without thermal insulation and heat-pipe diode mounting supports.

shutdown is initiated by turning off the condenser coolant, deploying the condenser block (i.e., the condenser block halves are removed from the diode), activating the condenser heater, and attaching the thermal insulation to the condenser.

### Experimental Results

A condenser temperature  $T_C$  has been defined as the average value of  $T_1$  and  $T_2$ , and a block temperature  $T_B$  has been defined as the average value of the evaporator thermal mass temperature  $T_9$  and the trap thermal mass temperature  $(T_{11} + T_{12})/2$ . The measured transient condenser and block temperatures are plotted in Figs. 3-5 together with the respective theoretical predictions. The experimental data are indicated by the symbol + for the mean condenser temperature  $T_C$  and \* for the mean block temperature  $T_B$ . Four cases have been investigated, viz., nominal condenser heat inputs of 5, 7.5, 10, and 15 W. In Figs. 6-8 both the experimentally determined and the theoretically predicted transient shutdown power curves are shown for the same heat input cases. In Table 2 the theoretically and experimentally determined shutdown energies are shown. The experimental results are discussed together with the theoretical predictions in the section on comparison between theory and experiment.

Systematic restart tests with the shutdown and overheated diode have not been carried out. In some cases, the diode was allowed to cool after termination of the shutdown test until it was in thermal equilibrium with the surroundings. Then a new shutdown test was carried out according to the procedure in the preceding section. In these cases the time period between subsequent shutdown tests was of the order of one to several hours. No problems were observed when establishing the forward-mode operation before initiation of shutdown. In other cases, the next shutdown test was carried out immediately after the previous one, the time period between the shutdown tests being between 20 min and 1 h. In these cases the diode was cooled by clamping the deployable condenser block tightly to the condenser section and switching on the condenser coolant loop. At the same time the evaporator and trap were heated with a fan, thus establishing the forward-mode operation before initiation of the next shutdown test. No problems concerning the restart of the diode were observed.

### Theory

Before describing the theoretical shutdown model employed, the diode shutdown mechanism shall be briefly described in a qualitative manner. In Fig. 9 two curves are indicated; one is  $\dot{Q}_{HP, \max} = f(m_1)$  (see also Ref. 5); the other is  $\dot{Q}_{IN}$ , the heat input to the condenser, which is held constant in the experiments. The intersection of the two curves is at time  $t = t_{DO}$ , which is the time when the diode starts to dry out. For  $t > t_{DO}$  the heat input to the condenser is larger than the maximum heat-transport capability of the heat pipe. The resulting transient mean temperatures for the condenser  $T_C$

and the evaporator plus trap block  $T_B$  are depicted in Fig. 10. For  $t > t_{DO}$  the heat transport from the condenser to the evaporator and trap is limited to the (decreasing) heat-pipe heat transport and the (increasing) heat transport by thermal conduction in the heat-pipe wall. Consequently, the block temperature  $T_B(t)$  is still rising but at a rate slower than for  $t < t_{DO}$ . The difference between the heat input and the heat transport by heat-pipe action/conduction causes the condenser temperature to rise in a steep slope. This rise continues until shutdown is accomplished at time  $t = t_{SD}$ . Then the rate of condenser temperature rise levels off, and both condenser and block temperature continue to rise at constant and similar rates. The shutdown process can thus be divided in two phases: One for  $0 \leq t \leq t_{DO}$  and the other for  $t > t_{DO}$ .

A mathematical model for transient diode shutdown is developed based on a heat-flow balance for two nodes, viz. condenser (mean condenser temperature  $T_C$ ) and evaporator plus trap block (mean block temperature  $T_B$ ). A schematic of

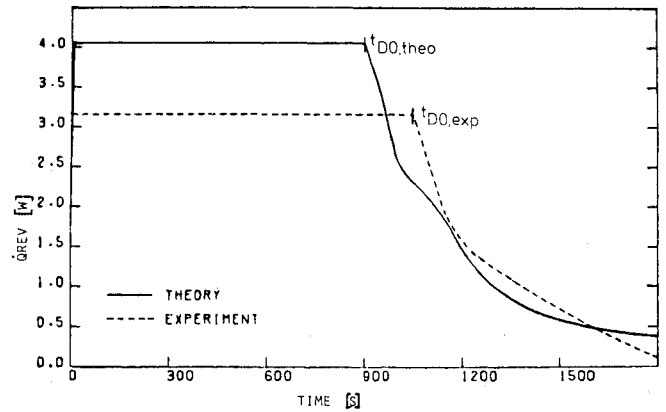


Fig. 6 Transient shutdown power for a nominal heat input to the condenser of 5 W.

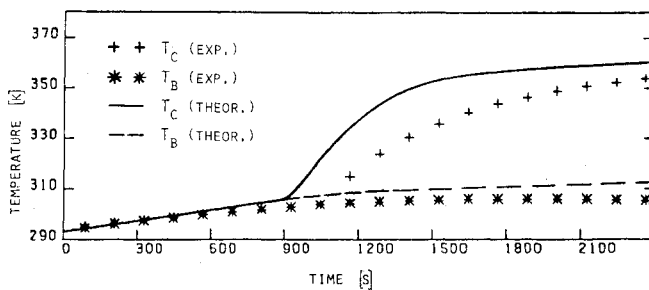


Fig. 3 Transient temperatures for heat-pipe diode shutdown with a nominal heat input to the condenser of 5 W.

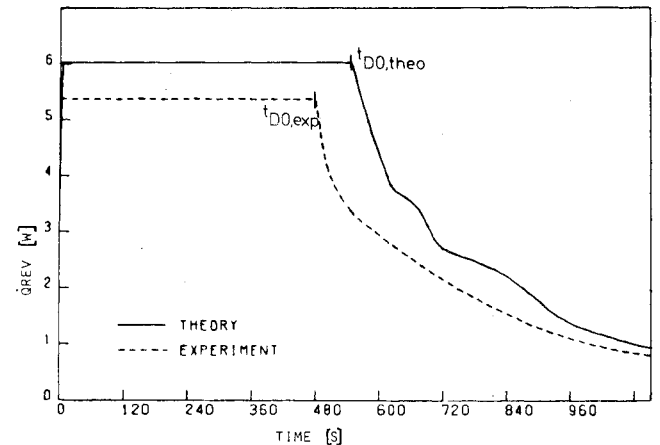


Fig. 7 Transient shutdown power for a nominal heat input to the condenser of 7.5 W.

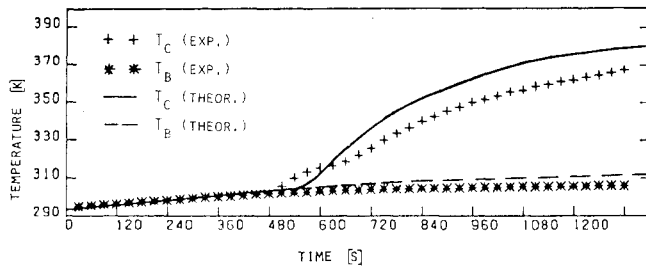


Fig. 4 Transient temperatures for heat-pipe diode shutdown with a nominal heat input to the condenser of 7.5 W.

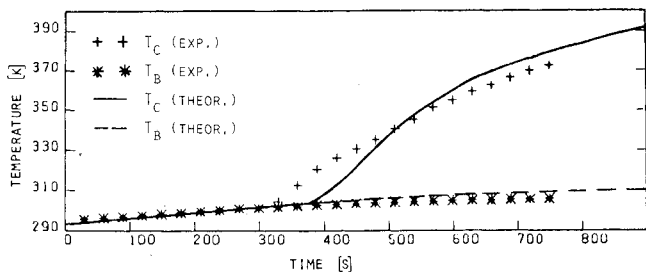


Fig. 5 Transient temperatures for heat-pipe diode shutdown with a nominal heat input to the condenser of 10 W.

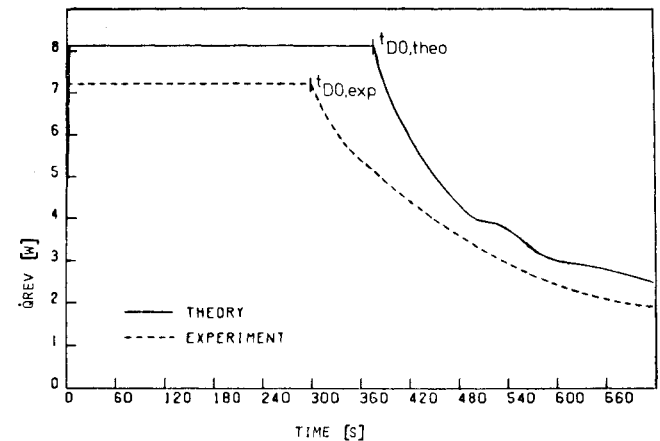


Fig. 8 Transient shutdown power for a nominal heat input to the condenser of 10 W.

Table 2 Summary of heat-pipe diode shutdown data

Heat input, $\dot{Q}_{IN}$ , W nominal	$t_{DO}$ , min		$t_{SD}$ , min Theory and exp.	$Q_{SD}$ , W·h	
	Theory	Exp.		Theory	Exp.
5	15	17.5	≈ 30	1.3	1.1
7.5	9.4	8	≈ 18.5	1.3	1.0
10	6.2	5.1	≈ 12	1.2	1.0
15	3.5	3	≈ 7	1.1	1.0

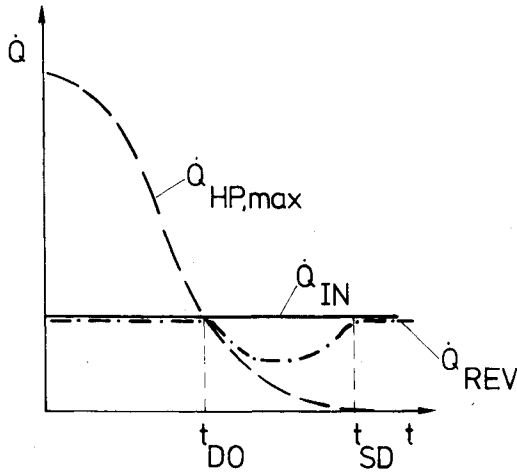


Fig. 9 Qualitative transient reverse-mode heat flow (without heat losses).

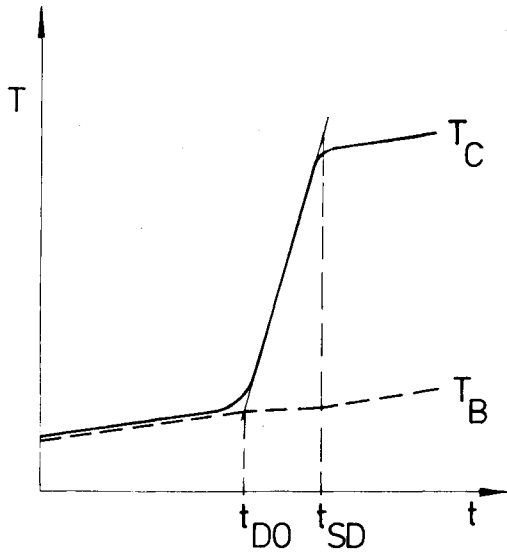


Fig. 10 Qualitative transient mean condenser and block temperatures (without heat losses).

the model is depicted in Fig. 11. The various symbols are defined as follows:  $T_C$  mean condenser temperature,  $T_B$  mean block temperature,  $\dot{Q}_{IN}$  heat input to condenser,  $\dot{Q}_{L,C}$  thermal losses from condenser due to free convection,  $\dot{Q}_{L,B}$  thermal losses from evaporator/trap block due to free convection,  $\dot{Q}_{SENS,C}$  sensible heat flow into condenser section,  $\dot{Q}_{SENS,AD}$  sensible heat flow into adiabatic section,  $\dot{Q}_{SENS,B}$  sensible heat flow into block,  $\dot{Q}_{HP}$  heat flow due to heat-pipe action,  $\dot{Q}_{COND}$  heat flow due to wall conduction.

A heat-flow balance for nodes  $T_C$  and  $T_B$  yields

$$\dot{Q}_{IN} = \dot{Q}_{HP} + \dot{Q}_{COND} + \dot{Q}_{SENS,C} + \dot{Q}_{L,C} \quad (1)$$

$$\dot{Q}_{HP} + \dot{Q}_{COND} = \dot{Q}_{SENS,AD} + \dot{Q}_{SENS,B} + \dot{Q}_{L,B} \quad (2)$$

The various heat flows are:

$$\dot{Q}_{IN} = \text{constant heat input to condenser}$$

$$\dot{Q}_{HP} = \begin{cases} C_F(T_C - T_B) & \text{for } 0 \leq t \leq t_{DO} \\ \dot{Q}_{HP,max} & \text{for } t > t_{DO} \end{cases} \quad (3a)$$

$$\dot{Q}_{HP,max} = f(m_I) \quad (\text{see Fig. 12})$$

$$\dot{Q}_{COND} = C_{REV}(T_C - T_B) \quad (4)$$

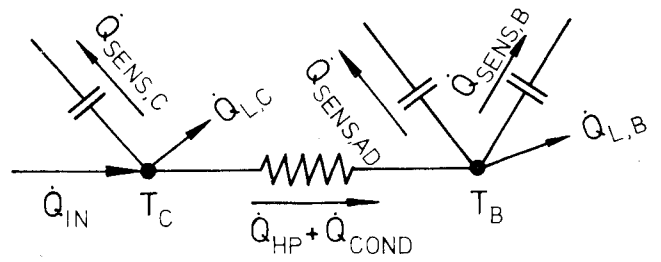


Fig. 11 Thermal model of transient shutdown of heat-pipe diode.

$$\dot{Q}_{SENS,C} = (CM)_C \frac{dT_C}{dt} \quad (5)$$

$$\dot{Q}_{SENS,AD} = (CM)_{AD} \frac{dT_{AD}}{dt}; \quad T_{AD} = \frac{1}{2}(T_C + T_B) \quad (6)$$

$$\dot{Q}_{SENS,B} = (CM)_B \frac{dT_B}{dt} \quad (7)$$

$$\dot{Q}_{L,C} = \begin{cases} 0 & \text{for } 0 \leq t \leq t_{DO} \\ F_C(T_C - T_{C,DO}) & \text{for } t > t_{DO} \end{cases} \quad (8a)$$

$$\dot{Q}_{L,C} = \begin{cases} 0 & \text{for } 0 \leq t \leq t_{DO} \\ F_C(T_C - T_{C,DO}) & \text{for } t > t_{DO} \end{cases} \quad (8b)$$

$$\dot{Q}_{L,B} = \begin{cases} 0 & \text{for } 0 \leq t \leq t_{DO} \\ F_B(T_B - T_{B,DO}) & \text{for } t > t_{DO} \end{cases} \quad (9a)$$

$$\dot{Q}_{L,B} = \begin{cases} 0 & \text{for } 0 \leq t \leq t_{DO} \\ F_B(T_B - T_{B,DO}) & \text{for } t > t_{DO} \end{cases} \quad (9b)$$

where  $(CM)_C$ ,  $(CM)_{AD}$ , and  $(CM)_B$  are the thermal masses of the condenser, adiabatic section, and evaporator plus trap, respectively;  $T_{AD}$  is the mean temperature of the adiabatic section;  $T_{C,DO}$  and  $T_{B,DO}$  are the mean condenser and block temperatures at time  $t_{DO}$ , respectively.

Since the diode is operated at an adiabatic temperature of about 20°C at the initiation of shutdown, the diode temperatures will rise above the temperature of the surroundings during the first phase of shutdown. Therefore, heat losses to the surroundings will occur. These heat losses are neglected in the theoretical model. However, the increasing heat losses during the second phase of shutdown, viz.,  $\dot{Q}_{L,C}$  from the condenser and  $\dot{Q}_{L,B}$  from the block, have been accounted for. The factors  $F_C$  and  $F_B$  in Eqs. (8b) and (9b), respectively, are the products of mean heat-transfer coefficients,  $h_C$  and  $h_B$ , and heat-transfer areas,  $A_C$  and  $A_B$ .

Equations (1) and (2) have to be solved simultaneously using Eqs. (3-9) to obtain the transient temperatures  $T_C$  and  $T_B$ . For  $0 \leq t \leq t_{DO}$ , this can be accomplished analytically (see Ref. 5), making use of the initial conditions:

$$T_C = T_B = 293 \text{ K} \quad \text{for } t = 0 \quad (10)$$

$$\dot{Q}_{IN} = \begin{cases} 0 & \text{for } t = 0 \\ \text{const} & \text{for } t > 0 \end{cases} \quad (11a)$$

$$\dot{Q}_{IN} = \begin{cases} 0 & \text{for } t = 0 \\ \text{const} & \text{for } t > 0 \end{cases} \quad (11b)$$

The constant heat inputs  $\dot{Q}_{IN}$  are 5, 7.5, 10, and 15 W, respectively.

For  $t > t_{DO}$ , Eqs. (1) and (2) have to be solved numerically. In addition, Fig. 10 has to be used and the following equations have to be employed to determine the liquid-fill charge in the heat pipe  $m_I$  at any time  $t$

$$m_I(t) = m_{tot} - \int_{t=0}^t \dot{m}_T(t) dt \quad (12)$$

$$\dot{m}_T(t) = a \frac{\dot{Q}_{HP}(t)}{h_{fg}} \quad (13)$$

where  $m_{tot}$  is the total initial liquid inventory of the heat pipe,  $\dot{m}_T(t)$  the mass flow into the trap which is trapped there,  $a$  a

factor defining the fraction of the condensed mass flow which is trapped in the trap (for unrestricted flow into the trap,  $a=0.69$ ), and  $h_{fg}$  the latent heat of vaporization of the working fluid.

From Eqs. (12) and (13)

$$m_I(t) = m_{\text{tot}} - \frac{a}{h_{fg}} \int_{t=0}^t \dot{Q}_{HP}(t) dt \quad (14)$$

Accounting for Eqs. (3) and (11) one obtains

$$m_I(t) = m_{\text{tot}} - \frac{a}{h_{fg}} \dot{Q}_{IN} t_{DO} + \int_{t=t_{DO}}^t \dot{Q}_{HP, \max}(t) dt \quad (15)$$

In Figs. 3-5 the theoretical curves for  $T_C$  and  $T_B$  are plotted together with the respective experimental data for the following heat inputs to the condenser: 5, 7.5, and 10 W. The theoretical curves have been obtained using an average heat-transfer coefficient  $h = h_C = h_B = 7 \text{ W/m}^2 \cdot \text{K}$ .

The transient shutdown power is calculated as

$$\dot{Q}_{REV}(t) = (CM)_B \frac{dT_B}{dt} \quad (16)$$

The shutdown energy  $Q_{SD}$  is determined using the following equation:

$$Q_{SD} = \int_{t=0}^{t_{SD}} \dot{Q}_{REV}(t) dt = (CM)_B \int_{t=0}^{t_{SD}} \frac{dT_B(t)}{dt} dt \quad (17)$$

The theoretical predictions are discussed together with the experimental results in the next section.

### Comparison Between Theory and Experiment

The transient mean condenser and block temperatures are depicted in Figs. 3-5 for the cases  $\dot{Q}_{IN} = 5, 7.5$ , and 10 W. The temperature at initiation of shutdown is 293 K. The agreement between theory and experiments is good during the first phase of shutdown ( $0 \leq t \leq t_{DO}$ ). For  $t > t_{DO}$  the agreement is also good concerning the block temperature  $T_B$ . It is not so good concerning the condenser temperature  $T_C$ . For the 5 and 7.5 W cases the predicted condenser temperature rises with a steeper slope and remains higher throughout shutdown. For the 10 W case the predicted condenser temperature starts to rise later than the experimental curve. Toward the end of shutdown the theoretical and experimental temperatures come close together. It is assumed that the discrepancies between theory and experiment can be explained by the fact that the thermal losses to the surroundings could not be adequately estimated.

In Figs. 6-8 the transient shutdown powers for the three nominal heat input cases of 5, 7.5, and 10 W are depicted. The experimental curves have been obtained from the measured transient block temperatures according to Eq. (16). The theoretical curves indicate that only part of the nominal heat input  $\dot{Q}_{IN}$  is transported through the diode to the block. This is due to various facts: 1) the diode wall material and the fluid inventory have to be heated; 2) there are losses from the condenser surface to the surroundings by convection and also by radiation and conduction; 3) the latter two losses have not been accounted for and are partly responsible for the difference between theoretical and experimental shutdown power curves. Nevertheless, the overall agreement between theoretical and experimental curves is good. However, there are some still unexplained discrepancies concerning details of the curve shape. They might be partially explained by the inherent precision problems which arise when  $\dot{Q}_{REV}$  [Eq. (16)] is determined. Minor changes in the slopes of the curves for  $T_B$  greatly affect the respective shutdown power.

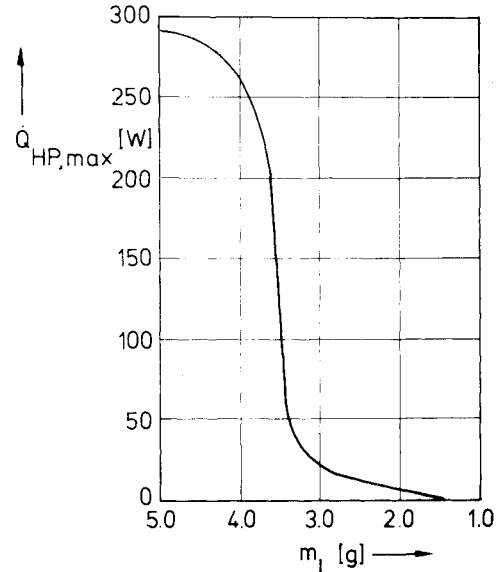


Fig. 12 Maximum heat-transport capability of aluminum axial-groove heat-pipe diode vs ammonia fill charge at 20°C.

The shutdown energies for the investigated cases are summarized in Table 2 together with other relevant shutdown data. They have been determined using Eq. (17). The agreement between theoretical predictions and experimental data is good. A comparison of the measured shutdown energy (approximately 1.0 W·h) with the minimum theoretical shutdown energy (1.48 W·h) indicates that the back-piping action during reversal is small. In fact the actual shutdown energies are smaller than the minimum theoretical value. This can be explained referring to Fig. 12. There it can be seen that for the axial-groove heat pipe the heat-pipe operation becomes essentially zero for a liquid inventory of about  $\leq 1, 5$  g, i.e., for still partially filled grooves. It should also be mentioned that the shutdown times have been determined for the situation when  $dT_B/dt=0$  and  $dT_C/dt=0$ . Because of the small variations in the shapes of the transient temperatures, the determination of the shutdown time is not extremely precise. If the shutdown times were to be determined to be somewhat longer, the associated shutdown energies would also become somewhat bigger.

Compared with results obtained from a different shutdown technique, viz., by cooling evaporator and trap while maintaining the condenser at a constant temperature,<sup>5,7</sup> the shutdown energy data are in good agreement. This holds only to a certain degree for the shutdown times  $t_{SD}$ . For the present experiments, they turn out to be strongly dependent on the shutdown condition applied (heat input  $\dot{Q}_{IN}$  to condenser). This has not been the case in the experiments of Refs. 5 and 7. There the shutdown times were constant (about 18 min) for all shutdown cases. The heat inputs to the condenser have been varied, too. However, they were controlled in such a way as to closely approximate the maximum heat-transport capability of the diode. This resulted in a high but short initial heat input to the condenser (the highest input was 110 W and applied for about 21 s, the smallest input was 36 W and applied for about 54 s), which soon leveled off and fell below 5 W (after about 4 min). Thus the previous experiments of Refs. 5 and 7 are approximately equivalent to the present experiments where the heat input to the condenser has been held constant at 5 W or somewhat higher. If one compares the shutdown case with  $\dot{Q}_{IN} = 7.5$  W (nominal), which corresponds to a real heat input of about 5.4 W (Fig. 4), the resulting shutdown time is about 18.5 min. It thus can be concluded that the different shutdown techniques lead to very similar results.

### Summary

The shutdown characteristics of an axial-groove liquid-trap heat-pipe thermal diode have been theoretically and experimentally determined employing a shutdown technique which consisted of heating the condenser section by means of a constant heat input to the condenser, while having both the evaporator and trap thermally free-floating. The overall agreement between predictions and experiments was good. However, a refinement of both the theoretical shutdown model as well as the measurement technique is desirable. This could lead to a more perfect understanding of the transient diode shutdown behavior. The comparison of the present data with those obtained from different shutdown tests showed that by proper interpretation of the test data, the agreement of the experimental data is good.

### Acknowledgment

This research has been supported under Contract 2993/76/NL/PP(SC) by European Space Research and Technology Center (ESTEC), Noordwijk, the Netherlands.

### References

- <sup>1</sup>Kosson, R.L., Quadri, J.A., and Kirkpatrick, J.P., "Development of a Blocking-Orifice Thermal Diode Heat Pipe," AIAA Paper 74-754, July 1974.
- <sup>2</sup>Brennan, P.J. and Groll, M., "Application of Axial Grooves to Cryogenic Variable Conductance Heat Pipe Technology," Paper E2, *Proceedings of the Second International Heat Pipe Conference*, ESA SP-112 (Preprint), Vol. 1, March-April 1976.
- <sup>3</sup>Swerdling, B. and Kosson, R., "Design, Fabrication and Testing of a Thermal Diode," Final Report, NASA CR-114526, Nov. 1976.
- <sup>4</sup>Quadri, J.A. and McCreight, C.R., "Development of a Thermal Diode Heat Pipe for Cryogenic Applications," AIAA Paper 77-192, Jan. 1977.
- <sup>5</sup>Groll, M., Münzel, W.D., Supper, W., and Savage, C.J., "Development of an Axial Groove Aluminum/Ammonia Liquid Trap Heat Pipe Thermal Diode," *Proceedings of the Third International Heat Pipe Conference*, Palo Alto, Calif., March-April 1978.
- <sup>6</sup>Williams, R.J., "Transient Shutdown Analysis of Low-Temperature Diodes," NASA TP 1369, March 1979.
- <sup>7</sup>Groll, M., Münzel, W.D., Supper, W., and Savage, C.J., "Transient Behavior of Liquid Trap Heat Pipe Thermal Diodes," AIAA Paper 79-1094, June 1979.

## *From the AIAA Progress in Astronautics and Aeronautics Series*

# SPACECRAFT CHARGING BY MAGNETOSPHERIC PLASMAS—v. 47

*Edited by Alan Rosen, TRW, Inc.*

Spacecraft charging by magnetospheric plasma is a recently identified space hazard that can virtually destroy a spacecraft in Earth orbit or a space probe in extra terrestrial flight by leading to sudden high-current electrical discharges during flight. The most prominent physical consequences of such pulse discharges are electromagnetic induction currents in various on-board circuit elements and resulting malfunctions of some of them; other consequences include actual material degradation of components, reducing their effectiveness or making them inoperative.

The problem of eliminating this type of hazard has prompted the development of a specialized field of research into the possible interactions between a spacecraft and the charged planetary and interplanetary mediums through which its path takes it. Involved are the physics of the ionized space medium, the processes that lead to potential build-up on the spacecraft, the various mechanisms of charge leakage that work to reduce the build-up, and some complex electronic mechanisms in conductors and insulators, and particularly at surfaces exposed to vacuum and to radiation.

As a result, the research that started several years ago with the immediate engineering goal of eliminating arcing caused by flight through the charged plasma around Earth has led to a much deeper study of the physics of the planetary plasma, the nature of electromagnetic interaction, and the electronic processes in currents flowing through various solid media. The results of this research have a bearing, therefore, on diverse fields of physics and astrophysics, as well as on the engineering design of spacecraft.

304 pp., 6 x 9, illus. \$16.00 Mem. \$28.00 List

TO ORDER WRITE: Publications Dept., AIAA, 1290 Avenue of the Americas, New York, N. Y. 10019